Hindawi Publishing Corporation
International Journal of Microwave Science and Technology
Volume 2014, Article ID 486051, 6 pages
http://dx.doi.org/10.1155/2014/486051

Research Article

Ultrawide Bandwidth 180°-Hybrid-Coupler in Planar Technology

Steffen Scherr, Serdal Ayhan, Grzegorz Adamiuk, Philipp Pahl, and Thomas Zwick

Institut für Hochfrequenztechnik und Elektronik, Karlsruhe Institute of Technology (KIT), Kaiserstraße 12, 76131 Karlsruhe, Germany

Correspondence should be addressed to Steffen Scherr; steffen.scherr@kit.edu

Received 3 February 2014; Revised 15 April 2014; Accepted 15 May 2014; Published 2 June 2014

Academic Editor: Yo Shen Lin

A new concept of an ultrawide bandwidth 180°-hybrid-coupler is presented. The ultrawideband design approach is based on the excitation of a coplanar waveguide (CPW) mode and a coupled slot line (CSL) mode in the same double slotted planar waveguide. The coupler is suitable for realization in planar printed circuit board technology. For verification of the new concept a prototype was designed for the frequency range from 3 GHz to 11 GHz, built, and measured. The measurement results presented in this paper show a good agreement between simulation and measurement and demonstrate the very broadband performance of the new device. The demonstrated coupler with a size of 40 mm × 55 mm exhibits a fractional bandwidth of 114% centered at 7 GHz with a maximum amplitude imbalance of 0.8 dB and a maximum phase imbalance of 5°.

1. Introduction

The main task of a 180°-hybrid-coupler is the division of an input signal into two autonomous signals, which possess the same amplitude and are in-phase or out-of-phase. The phase relation between the output signals depends on the feeding port, referred to as Σ-port or Δ-port, respectively. A 180°-hybrid-coupler consists all in all of four ports, two inputs and two outputs. The division into in-phase signals introduces a principle of a basic power divider, which can be easily realized even for very large bandwidths. The creation of differential signals can be achieved by a differential power divider. Bialkowski and Abbosh [1] describe such a differential power divider for UWB technology. A 180°-hybrid-coupler combines the two aforementioned power dividing principles in one single device.

180°-hybrid-couplers are used in many microwave circuits such as push-pull amplifiers [2], balanced mixers [3], and pattern diversity antennas [4]. A further application of such couplers is in the monopulse radar technique, where sum and difference beams are created for an accurate angular tracking of the target [5]. The possibility of the creation of a sum and difference beam over UWB bandwidth is verified by the authors in [6].

The general advantage of the 180°-hybrid-coupler over conventional or differential power dividers is the possibility to process sum and differential signals in the same device. In narrowband systems, those kinds of couplers are well known as rat-race couplers or magic-tees. However, there is a demand for systems combining the new broadband possibilities (e.g., UWB technology) with traditional narrowband concepts (e.g., monopulse radar) [7]. Hence, hybrid-couplers that cover the UWB frequency band, for example, from 3 GHz to 11 GHz are of interest [8]. As traditional hybrid-coupler designs need wavelength-dependent structures, it is necessary to find wideband design approaches.

The presented coupler can be fabricated in planar technology or low temperature cofired ceramics (LTCC) to cover the aforementioned frequency band. Even on-chip fabrication in standard silicon technologies at mm-wave is possible with the new concept.

The coupler should possess a satisfactory impedance matching at the Σ- and Δ-port, low coupling between the Σ- and Δ-port, and high transition from the Σ- and Δ-port to the outputs. Under ideal conditions the amplitudes of the signals at the output ports are equal and the phase difference

is 0° when fed at the Σ-port and 180° when fed at the Δ-port. All port impedances are optimized to 50 Ω in the presented approach.

The following sections present the principle of the new coupler concept and the measurements which validate the functionality of the coupler.

2. Principle of the Coupler

Figure 1 shows the structure of the coupler. The dark gray and the light gray areas mark the metallization at the top of the coupler and at the bottom, respectively. For the explanation of the coupler's functioning port 1 (Σ-port) and port 2 (Δ-port) are considered as input ports, whereas port 3 and port 4 are output ports if one of the input ports is excited (Figure 1). The principle of the coupler can best be explained if the behavior of signals separately excited at port 1 and port 2 on their way to port 3 and port 4 is described.

At first the behavior of signals coupled into port 1 (Σ-port) is investigated. An excitation of port 1 leads to signals having the same amplitude and phase at the outputs. The corresponding simplified electric field distribution is depicted in Figure 1(a), showing the signal propagation from port 1 to port 3 and to port 4. The CPW mode [4] is excited in the two adjacent slots and the signal is further transferred through the set of vias. The vias realize a short circuit of the outer coplanar waveguide metallizations by connecting a metallized patch, placed on the opposite side of the substrate. As a CPW line is formed by a conductor with a separated pair of ground planes, there is no change in the potential introduced by the vias. The CPW mode can pass the vias without interruption. Behind the vias the slot lines cross the microstrip line, which is placed on the top side of the coupler. The electric field is concentrated mainly in the slots, that is, at the top of the coupler; hence, the influence of the microstrip line on the transmission of the CPW mode can be neglected. The power divider is realized by separating the adjacent slots of the coplanar waveguide into separate slot lines. To avoid an abrupt impedance change, the coplanar waveguide before the power divider is tapered. At the end of each of the slot lines an aperture coupling transfers the signals to the microstrip lines [14]. As can be seen from Figure 1(a), the direction of the electric field components at the outputs is the same. Thus, the output signals are in-phase. Due to the design of the hybrid-coupler, the output signals possess the same amplitude if a CPW mode is excited at the Σ-port, for example, by an SMA connector.

If a signal is coupled into port 2 (Δ-port), the signals at port 3 and port 4 are differential to each other. The signal travels from the Δ-port to the aperture coupling at the end of the microstrip line (Figure 1(b)). The aperture coupling of the signal causes an excitation of the CSL mode [4] in the adjacent slot lines. This form of the coupling is similar to the traditional one [14]; however, in the proposed structure two adjacent slots are used instead of a single one. By proper adjustment of the aperture coupling both slots get excited with electric fields that are oriented in the same direction (Figure 1(b)). A hybrid-coupler isolates the Σ-port and the Δ-port from each other. This isolation is realized by the implementation of the vias. In contrast to the CPW mode, the CSL mode sees a different potential at the ground planes. Hence, the short circuit caused by the vias blocks the CSL mode. In succession the signal propagated in this CSL mode is reflected. This effect is similar to the reflection at the slot widening in the traditional wideband transition from microstrip line to slot line [14]. As the set of vias allows the transition of the CPW mode and reflects the CSL mode, the vias serve as a mode filter. In order to achieve a higher reflection of the CSL mode, three sets of vias are used. The CSL mode is transmitted through the slot separation to the aperture couplings and finally to port 3 and port 4. The signals at these ports are out-of-phase. In order to guarantee the equality of the amplitudes at port 3 and port 4 both slots have to be excited with the same amplitude. This can be achieved by a proper optimization of the slots' relative orientation with respect to the coupling microstrip line. Furthermore, the distance between the slots should be kept small; otherwise, it is impossible to excite the slots with equal signals.

3. Proposed UWB 180°-Hybrid-Coupler

The coupler is built on Duroid 4003 with a thickness of $h_{\text{sub}} = 0.79$ mm and a dielectric constant of $\epsilon_r = 3.55$. The dimensions of the prototype (Figures 2 and 3) are 40 mm × 55 mm. As the microstrip lines and the coplanar lines do not limit the bandwidth of the coupler [15], the only components with a frequency dependent and hence bandwidth limiting geometry are the aperture couplings. Therefore, the main objective of the optimization for this coupler is to optimize the wideband microstrip line to coplanar line transition. Simulations (CST Microwave Studio [16]) show that the best results can be achieved, if the width of the coplanar line at this transition is minimized. In this case the transition in combination with the vias behaves like a traditional aperture coupling from microstrip line to single slot line.

A width of 60 μm for the slot of the coplanar line is chosen at the microstrip line to coplanar line transition. Since this part is very sensitive to etching tolerances, a smaller slot width could lead to strong deviations between simulation and measurement. A slot width of less than 60 μm would be advantageous, but it results in very low yield for the applied etching process. However, a further miniaturization of this part of the coupler and the possibility to use a substrate with a higher dielectric constant (e.g., LTCC fabrication) would lead to a better overall performance. After the slot size and the impedance of the coplanar line are determined, the width can be calculated to 0.35 mm [15]. All port impedances are optimized for 50 Ω and the size of the microstrip line and the coplanar line is limited by the size of the connectors. Hence, tapers are used to achieve wideband behavior while providing a solderable geometry at the connectors. The width of the slot line at the end of the coplanar line determines the matching of the CSL and the CPW mode. A larger width of the slot line improves the matching of the CSL mode and a smaller width of the slot line improves the matching of the CPW mode. As a trade-off, a width of 0.26 mm is selected here. The aperture

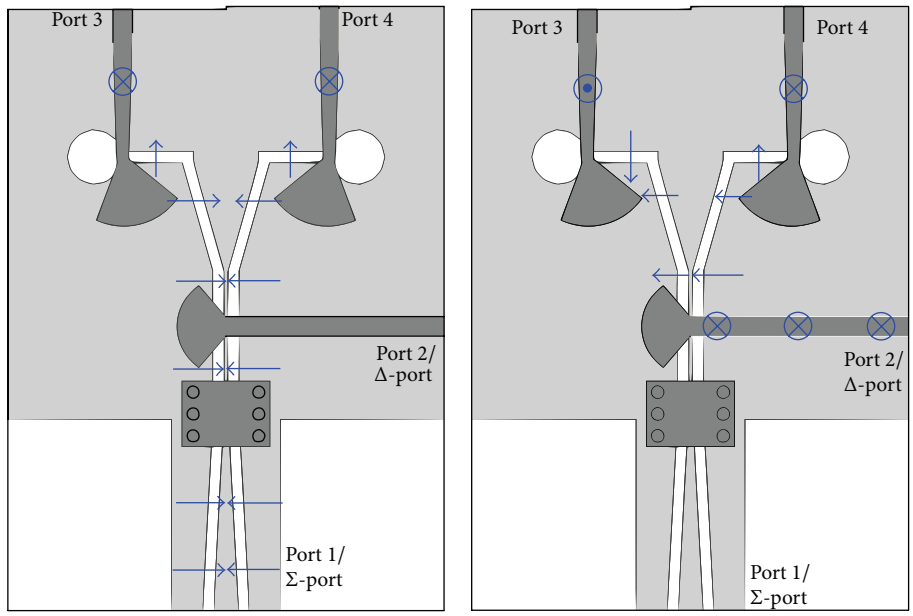

(a) Feeding at Σ-port (b) Feeding at Δ-port

Figure 1: Schematical electric field distribution in the coupler. The slot lines are enlarged to get a better understanding of the coupler's principle.

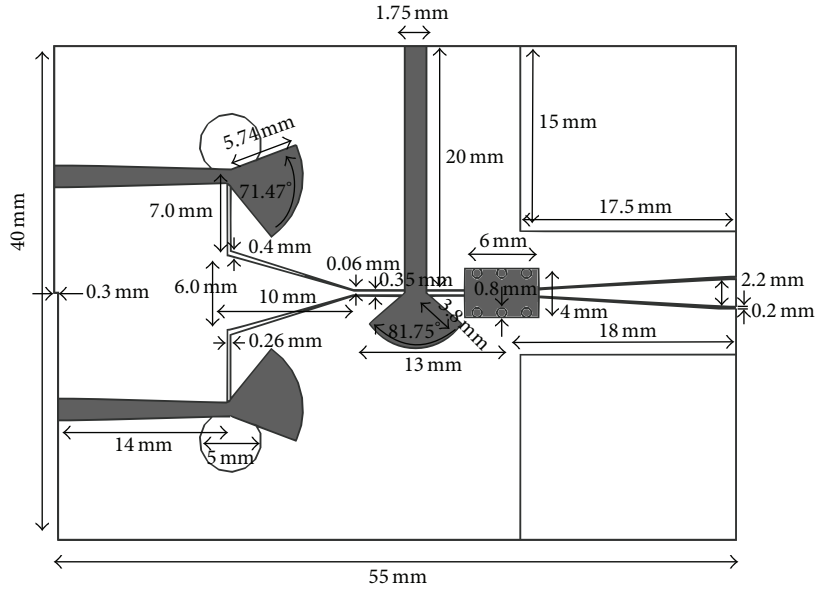

Figure 2: Size of the hybrid coupler.

couplings from microstrip line to slot line are realized by $\lambda/4$-stubs (5.3 mm at 7.5 GHz, Figure 2), which are extended to circles and segments of circles to increase the bandwidth [6, 14, 15].

4. Simulation and Measurement Results

The three most important parameters of a hybrid-coupler are the S-parameters, the amplitude imbalance, and the phase difference, which will be considered in this section. Figure 4 shows the simulated and measured amplitudes of the S-parameters of the coupler. The coupler exhibits an ultrabroadband behavior in the frequency range from 3 GHz to 11 GHz.

The input impedance matching at port 1 and port 2 as well as the decoupling between the ports is sufficient in the desired frequency range. The transmission factor from port 1 (Σ-port) to port 3 is close to the optimum value of −3 dB in the lower frequency range and decreases slightly with increasing frequency. The transmission from port 2 (Δ-port) to port 3

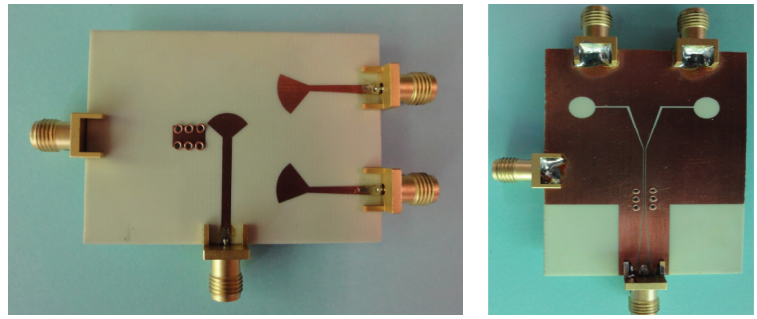

(a) Top view (b) Bottom view

Figure 3: Photograph of the prototype.

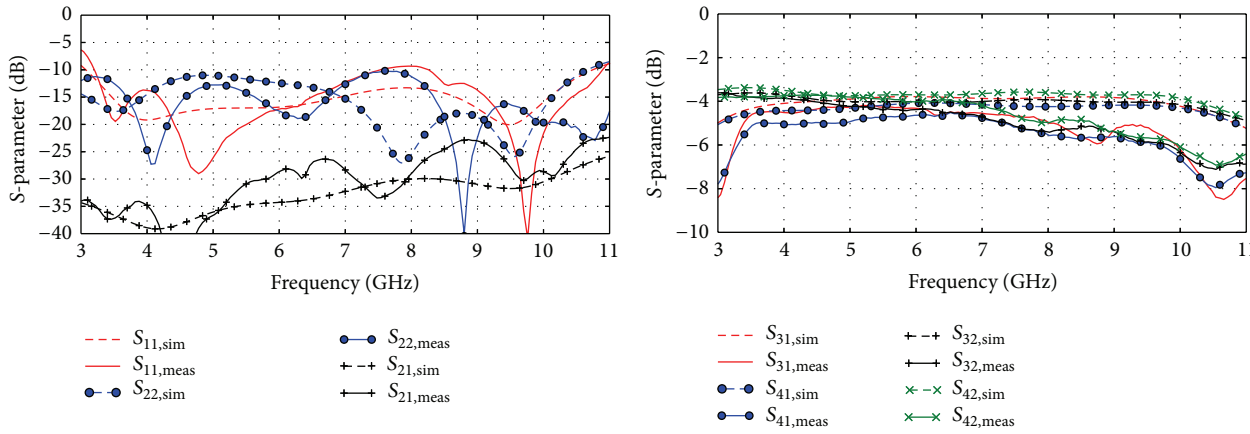

(a) S_{11}, S_{22}, and S_{21} (b) S_{31}, S_{41}, S_{32}, and S_{42}

Figure 4: Simulated and measured amplitudes of the S-parameters of the presented coupler.

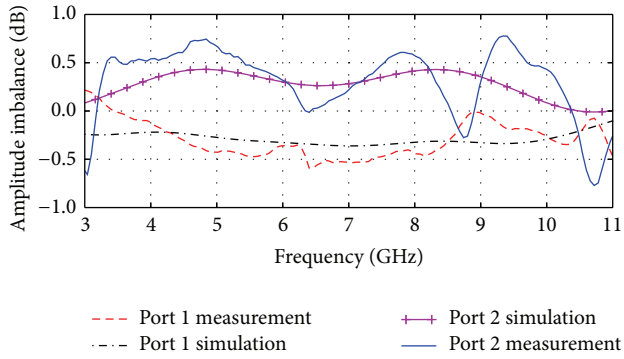

Figure 5: Amplitude imbalance of the output signals for feeding at port 1 and port 2.

encounters similar losses in the high frequency range. The simulations show that these losses are mainly caused by radiation. They can be decreased by using a substrate with lower thickness h_{sub} and higher dielectric constant ϵ_r or by implementing the coupler in LTCC technology. Due to the lossless materials assumed in the simulation, the measured transmission losses are slightly different compared to the simulated losses. Above 7 GHz increased losses have been observed due to tolerances in the manufacturing process at the microstrip line to coplanar line transition.

The measured amplitude imbalance curves are shown in Figure 5. The imbalance is calculated between the output signals by exciting separately port 1 (Σ-port) and port 2 (Δ-port) and calculating the relation of the S-parameters at the output ports, respectively. For the feeding at port 1, smaller differences in the amplitudes (max. 0.6 dB) are observed than for port 2 (max. 0.8 dB). This is mainly due to the less complicated excitation procedure of the CPW mode. Based on the presented curves, it can be concluded that the coupler possesses a good amplitude behavior over the UWB frequency range.

In 180°-hybrid-couplers the phase behavior of the transmission factors is crucial. Figure 6 shows the simulated and measured phase differences between the outputs of the coupler for separate feeding at port 1 and port 2. The values of the phase difference, while port 1 (Σ-port) is excited, are relatively small and do not exceed 3.5°. During the excitation of the Δ-port, the phase imbalance has shown a linearly increasing error over frequency. This has been compensated

Table 1: Comparison between planar 180°-hybrid-couplers.

Reference	Relative bandwidth B%	Center frequency f_c	Maximal amplitude imbalance	Maximal phase imbalance	Size [mm]	Layers
[9]	60%	2 GHz	0.2 dB	2°	—	2
[10]	69%	10.1 GHz	0.6 dB	1.0°	20 × 30	2
[11]	100%	4 GHz	0.4 dB	2.5°	—	1
[12]	100%	4 GHz	0.4 dB	4°	—	1
[13]	100%	6 GHz	—	—	24 × 35	2
This work	114%	7 GHz	0.8 dB	5°	40 × 50	2

Note: the values are partly estimated from figures if not explicitly given in the paper.

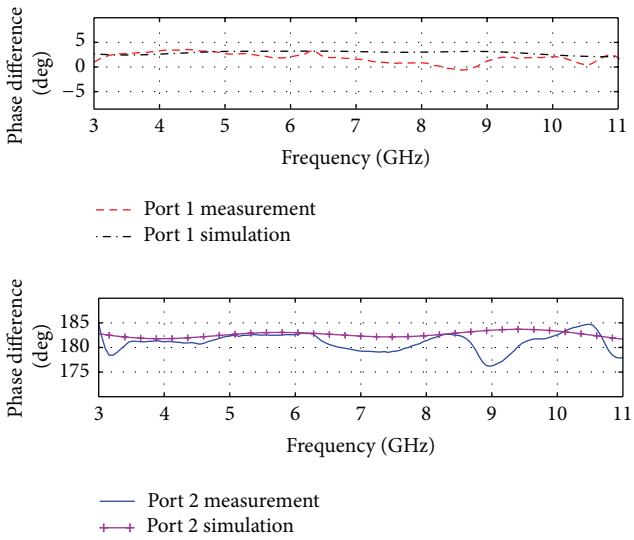

Figure 6: Phase difference of the output signals for feeding at port 1 and port 2.

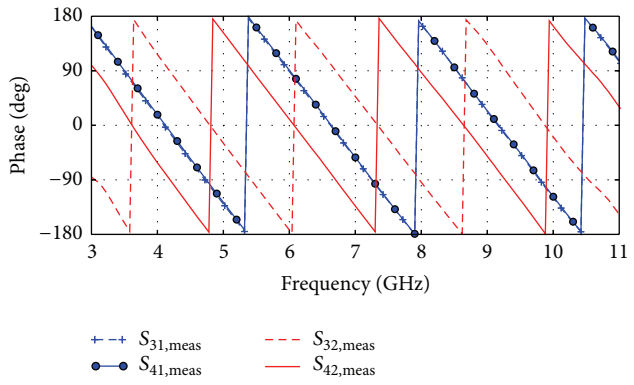

Figure 7: Measured phase response of the hybrid coupler.

by an adjustment of the length of the microstrip line at port 4 (Figures 1 and 2). The linear dependency of the phase imbalance on the frequency is due to the different arrangements of both slot lines with respect to the microstrip line coming from port 2. The phase balance when this port is excited can be improved, for example, by a closer arrangement of the adjacent slot lines; however, the compensation of the nonideality is still necessary in the presented design. Due to the extension of the microstrip line at port 4, the phase deviations do not exceed 5° for feeding at the Δ-port.

Table 1 compares the performance of different planar 180°-hybrid-couplers. The relative bandwidth is defined as

$$\mathrm{B\%} = 2 \cdot \frac{f_h - f_l}{f_h + f_l} \cdot 100 = \frac{f_h - f_l}{f_c} \cdot 100, \quad (1)$$

where f_h and f_l are the highest and lowest frequency, which cover a frequency band in which the coupler possesses a return loss of mostly less than −10 dB and an amplitude imbalance of less than 1 dB. It can be found that the proposed 180°-hybrid-coupler is better than the referenced ones in terms of relative bandwidth. Compared to the other couplers, the new coupler covers the whole UWB frequency band defined by the FCC and can be used for high resolution applications. All subcomponents of the coupler (aperture couplings, line separation, vias, etc.) maintain a nearly linear phase response (Figure 7). Hence, the coupler can also be applied to pulse-based UWB systems (IR-UWB), where a small distortion of the pulse is desired [1, 6, 17].

5. Conclusions

A concept for the realization of a UWB 180°-hybrid-coupler in planar technology requiring only two metal layers is presented. This concept is verified by measurements of the prototype, which is optimized for the frequency range from 3 GHz to 11 GHz. Across this frequency range, the return loss for the Δ-port is mostly less than −10 dB and always better than −10 dB at the Σ-port. The maximal phase imbalance for the Σ-port and the Δ-port is 3.5° and 5°, respectively, and the maximal amplitude imbalance is 0.6 dB and 0.8 dB, respectively. The linear phase response of the coupler allows the cost-effective usage for pulse-based UWB systems. The presented prototype can be applied to many applications where ultrawide bandwidth is desired in the creation of in-phase and differential signals, for example, the monopulse radar principle in a combination with the UWB technique.

Conflict of Interests

The authors declare that there is no conflict of interests regarding the publication of this paper.

References

[1] M. E. Bialkowski and A. M. Abbosh, "Design of a compact UWB out-of-phase power divider," *IEEE Microwave and Wireless Components Letters*, vol. 17, no. 4, pp. 289–291, 2007.

[2] S. Toyoda, "Broad-band push-pull power amplifier," in *Proceedings of the IEEE MTT-S International Microwave Symposium Digest*, vol. 1, pp. 507–510, May 1990.

[3] R. Blight, "Microstrip hybrid couplers and thier integration into balanced mixers at X and K-bands," in *Proceedings of the G-MTT International Microwave Symposium Digest*, pp. 136–138, Boston, Mass, USA, May 1967.

[4] E. Gschwendtner and W. Wiesbeck, "Ultra-broadband car antennas for communications and navigation applications," *IEEE Transactions on Antennas and Propagation*, vol. 51, no. 8, pp. 2020–2027, 2003.

[5] M. Skolnik, *Introduction to Radar Systems*, McGraw-Hill, New York, NY, USA, 1962.

[6] G. Adamiuk, W. Wiesbeck, and T. Zwick, "Multi-mode antenna feed for ultra wideband technology," in *Proceedings of the IEEE Radio and Wireless Symposium (RWS '09)*, pp. 578–581, San Diego, Calif, USA, January 2008.

[7] G. Adamiuk, C. Heine, W. Wiesbeck, and T. Zwick, "Antenna array system for UWB-monopulse-radar," in *Proceedings of the International Workshop on Antenna Technology (iWAT '10)*, pp. 1–4, Lisbon, Portugal, March 2010.

[8] Federal Communications Commission (FCC), "Revision of part 15 of the commissions rules regarding ultrawideband transmission systems," First Report and Order, ET Docket 98-153, FCC 02-48, 2002.

[9] J.-P. Kim and W. S. Park, "Novel configurations of planar multilayer magic-T using microstrip-slotline transitions," *IEEE Transactions on Microwave Theory and Techniques*, vol. 50, no. 7, pp. 1683–1688, 2002.

[10] K. U-yen, E. J. Wollack, J. Papapolymerou, and J. Laskar, "A broadband planar magic-T using microstrip-slotline transitions," *IEEE Transactions on Microwave Theory and Techniques*, vol. 56, no. 1, pp. 172–177, 2008.

[11] L. Fan, C.-H. Ho, S. Kanamaluru, and K. Chang, "Wide-band reduced-size uniplanar magic-T, hybrid-ring, and de Ronde's CPW-slot couplers," *IEEE Transactions on Microwave Theory and Techniques*, vol. 43, no. 12, pp. 2749–2758, 1995.

[12] B. R. Heimer, L. Fan, and K. Chang, "Uniplanar hybrid couplers using asymmetrical coplanar striplines," *IEEE Transactions on Microwave Theory and Techniques*, vol. 45, no. 12, pp. 2234–2240, 1997.

[13] M. E. Bialkowski and Y. Wang, "Wideband microstrip 180° hybrid utilizing ground slots," *IEEE Microwave and Wireless Components Letters*, vol. 20, no. 9, pp. 495–497, 2010.

[14] M. M. Zinieris, R. Sloan, and L. E. Davis, "A broadband microstrip-to-slot-line transition," *Microwave and Optical Technology Letters*, vol. 18, no. 5, pp. 339–342, 1998.

[15] K. Gupta, *Microstrip Lines and Slotlines*, Artech House, Norwood, Mass, USA, 2nd edition, 1996.

[16] CST Microwave Studio, http://www.cst.com.

[17] W. Sörgel and W. Wiesbeck, "Influence of the antennas on the ultra-wideband transmission," *EURASIP Journal on Applied Signal Processing*, vol. 2005, no. 3, Article ID 843268, 2005.